8B.4

3D RADIATIVE TRANSFER IN THE COMPLEX TOPOGRAPHY OF THE ARIZONA METEOR CRATER

Sebastian W. Hoch [a*], Bernhard Mayer [b] and C. David Whiteman [a]

[a] University of Utah, Salt Lake City, Utah, USA
[b] Deutsches Zentrum für Luft- und Raumfahrt (DLR), Oberpfaffenhofen, Germany

1. INTRODUCTION

Radiative transfer plays a key role in the energy exchange between the earth's surface and the atmosphere. Many models exist to simulate this exchange for the highly idealized case of a homogeneous atmosphere overlying a homogeneous surface. It is well known, however, that the radiative exchange of energy is further complicated by a more complex interface that is introduced by complex topography and varying surface properties: Shadows are cast by taller objects blocking direct solar radiation, diffuse radiation can be amplified due to reflecting surrounding terrain, solar radiation strongly varies on slopes with different exposure, and topography can block the emission of longwave radiation. All of these effects lead to the formation of different microclimates in mountainous terrain (Matzinger et al. 2003, Whiteman et al. 1989). These effects are not taken into account in many current boundary layer and mesoscale flow models.

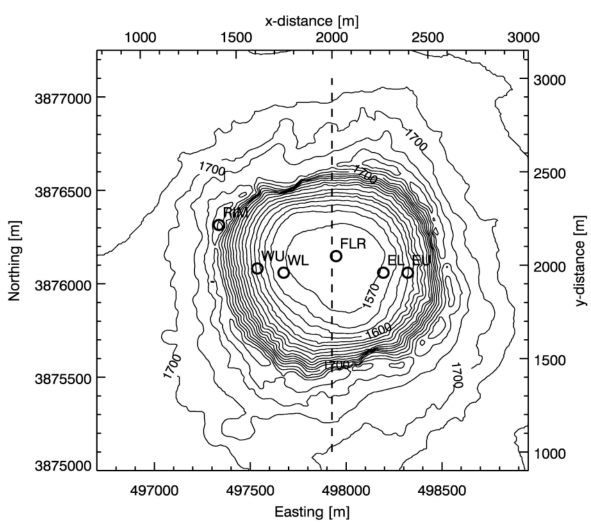

Fig. 1: Topographic map (left) showing the radiation measurement sites within the crater. The dashed line shows the location of the flux transect discussed later.

In recent years, three-dimensional radiative transfer models based on Monte Carlo photon tracing techniques have been developed to model radiative transfer in inhomogeneous cloudy atmospheres. One of these models, MYSTIC, also includes the physics and coding necessary to handle complex surface boundary conditions including topography and variable surface albedo (Mayer 1999, Mayer and Kylling 2000).

This paper uses detailed observations collected in the complex topography of the Arizona Meteor Crater during the recent METCRAX 2006 meteorological experiment (Whiteman et al. 2008) to validate MYSTIC for radiative transfer simulations within 3-dimensional topography. MYSTIC is then used in two simple parametric studies to investigate the role of surface-air temperature discontinuities and temperature stratification on the longwave radiative fluxes in the crater topography.

2. OBSERVATION SITES AND INSTRUMENTATION

During METCRAX 2006, extensive radiation data were collected in a unique, idealized topographic basin formed by the impact of a meteorite 50,000 years ago on the Colorado Plateau, 40 km east of Flagstaff, Arizona (Hoch and Whiteman 2007). Detailed observations of the shortwave and longwave components of the surface radiation budget were made at six different sites during METCRAX 2006 (Fig. 1). Two of the sites, one on the crater floor (FLR) and one on the crater rim (RIM), were located over quasi-horizontal surfaces. The remaining four sites were located on the sloping crater sidewalls, two on the west slope (West Upper, WU, and West Lower, WL) and two on the east slope (East Upper, EU, and East Lower, EL). For the six sites in the crater, the four main components of the radiation balance (shortwave incoming, shortwave reflected, longwave incoming and longwave outgoing radiation) were measured individually, quasi-parallel to the slope of the underlying terrain, using Eppley PSP or Kipp & Zonen CM21 pyranometers and Eppley PIR or Kipp & Zonen CG4 pyrgeometers. At the slope sites, the instruments were oriented parallel to the underlying slope as estimated by eye over a slope area of 10s of meters around the radiometer. The inclination and azimuth angles of the radiometer were then carefully measured and recorded. Further, diffuse radiation was measured at the crater rim and floor sites with LiCor pyranometers and shadowbands. All instrumentation was supplied and installed by the National Center for Atmospheric Research (NCAR). The radiative measurements were made at their Integrated Surface Flux Facility (ISFF) and Integrated Sounding System (ISS) sites.

*Corresponding author address: Sebastian W. Hoch, Univ. of Utah, Dept. of Meteorology, Salt Lake City, UT 84112; e-mail: sebastian.hoch@utah.edu

3. THE 3D RADIATIVE TRANSFER MODEL MYSTIC

MYSTIC (**M**onte Carlo code for the ph**ys**ically correct **t**racing of photons **i**n **c**loudy atmospheres) is capable of radiative transfer calculations in three-dimensional atmospheres (Mayer 1999, Mayer and Kylling 2000). The model, developed as a solver for the freely available uvspec/libRadtran (Mayer and Kylling 2005) packages handles three-dimensional clouds, inhomogeneous surface albedo, and topography. The accuracy of MYSTIC has been demonstrated previously by comparison with the one-dimensional DISORT code and with other three-dimensional solvers during the I3RC (intercomparison of 3D radiation codes) campaign, where deviations of less than 1% were found for well-defined conditions (Mayer 1999). For our comparison with data, MYSTIC was modified so that solar and thermal calculations could be made for arbitrarily oriented instruments, including the slope-parallel orientations required for energy considerations. A new backward Monte Carlo technique was implemented in MYSTIC to allow faster calculations of radiance and irradiance for the few sites where radiation measurements were made at Meteor Crater. Our calculations used a topographic domain of 4 x 4 km, with a horizontal grid resolution of 10 m. Figure 1 shows a centered cut-out of the topography. For every flux calculation, $1 \cdot 10^6$ photons were traced. The isotropic reflectivity factors used for the different sites were determined from the monthly mean observed albedos at these individual sites.

4. COMPARISONS

The clear sky day of 21 October 2006 was selected for the comparison of observed and modeled solar fluxes using the AFGL mid-latitude standard atmosphere as atmospheric model input.

The night of 22 - 23 October 2006 was chosen for the comparison of modeled and observed longwave fluxes. During this night, atmospheric profiles of temperature and humidity were available from three-hourly radiosonde ascents between 15 and 09 MST. These profiles, combined with those collected from tethersonde flights and a 10 m meteorological mast at the crater floor were used as input data sets for the model calculations.

4.1 Shortwave Fluxes

The modeled downward shortwave components of the radiation balance include direct and diffuse solar radiation. The modeled components were compared to observations at the crater floor (Fig. 2). There, prominent shadows cast from the surrounding crater rim strongly affect the radiation field in the morning and afternoon, a feature simulated by the model. The sum of the downward direct and diffuse components (global radiation), shortwave reflected radiation and albedo (the ratio between shortwave reflected and global radiation) can be compared at all sites.

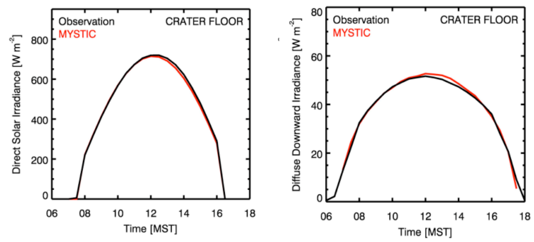

Fig. 2: Comparison of observed (black) and modeled (red) shortwave direct irradiance (left) and diffuse irradiance (right) at the crater floor for 21 October 2006.

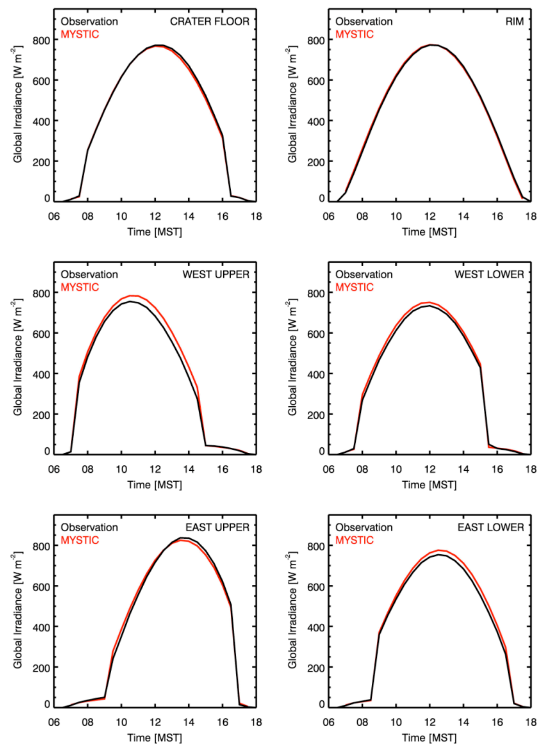

Fig. 3: Comparison of observed (black) and modeled (red) global radiation at the six sites in the crater for 21 October 2006.

The agreement between the observed and modeled direct and diffuse solar radiation is excellent. The curves overlap at most times. The topographic effect of *terrain shading* is very well reproduced with MYSTIC. The morning shading by the east rim and the afternoon shading by the west rim both match well with the observations.

Global radiation (Fig. 3) is symmetric about solar noon at the crater floor and rim, where the instruments were mounted horizontally. The asymmetry of the diurnal variation of global radiation at the sloping sites – the maximum global radiation is received prior to solar noon on the west sidewall and after solar noon on the east sidewall – is well represented by the MYSTIC calculations. The topographic influence on the radiation balance by *terrain exposure* (slope and azimuth angle) is very well reproduced with MYSTIC. In addition, the timing of the morning and evening shadows, which strongly affect the magnitude of global radiation, matches well with the observations.

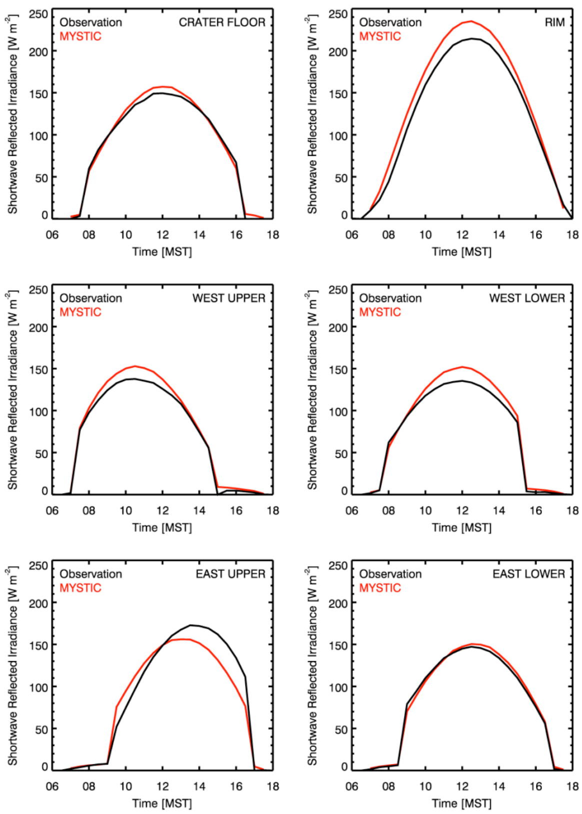

Fig. 4: Comparison of observed (black) and modeled (red) short-wave reflected radiation at the six crater sites for 21 October 2006.

Figure 4 compares the diurnal variation of observed and modeled shortwave reflected radiation. The model calculation is influenced by the choice of the isotropic reflectance factor that is prescribed for each model run. A value of 0.2 was used for all calculations, with the exception of the crater rim site, where 0.3 was chosen. These values were determined from the observed mean albedo at the sites. The use of these values with MYSTIC yielded shortwave outgoing fluxes that are slightly higher than those observed at most sites. With the exception of the East Upper site, however, MYSTIC realistically reproduced the site-specific diurnal variation seen in the observations. At East Upper, the influence of the site exposure was slightly underestimated, which may partly be due to a misrepresentation of the instrument measurement plane or due to a misrepresentation of the true local topography by the relatively coarse digital elevation model.

Figure 5 compares the diurnal variations of observed and modeled albedo for two selected sites, Rim and Floor. This comparison is an even more rigorous test: Mismatches in both global radiation and shortwave reflected radiation will influence albedo, defined as their ratio. The model reproduced the smooth diurnal albedo cycle at the Floor site as well as the distinctive shape of the diurnal albedo curve at the Rim site. At the Rim, MYSTIC successfully traces the effect of the – in the larger scale – westward sloping surface under a horizontal instrument plane. On the other hand, the mismatch in the reflected shortwave radiation previously mentioned at East Upper led to a mismatch of the diurnal albedo pattern (not shown). Despite the relatively crude terrain resolution, MYSTIC is shown to successfully simulate the effects of topography on the diurnal cycle of albedo.

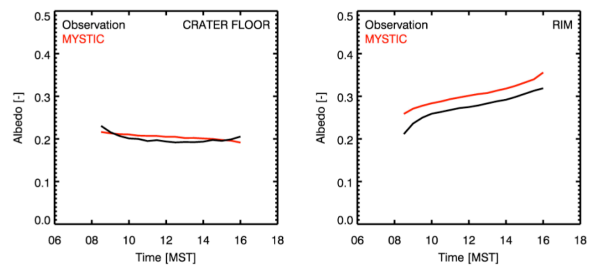

Fig. 5: Comparison of observed (black) and modeled (red) albedo at the crater floor and rim sites for 21 October 2006.

4.2 Longwave Fluxes

Atmospheric profiles used as input for the MYSTIC longwave calculations were obtained from data collected during METCRAX. Half-hourly means of the temperature and humidity profiles from the 10 m meteorological tower on the crater floor were combined with the sounding data of the central tethersonde inside the crater and the 3-hourly radiosonde profiles obtained just outside the crater. The modeled longwave fluxes were then compared with 30-minute mean radiation measurements. For the MYSTIC calculations, the atmospheric profiles of temperature and humidity were assumed to be invariant across the crater from sidewall to sidewall, with the ground temperature being equal to the air temperature at that elevation. In future work, it will be possible to input a grid of surface temperatures. The present simulations thus do not take into account the shallow stable atmospheric layers that were observed over the crater sidewalls, something that we hope to improve in future work.

Figures 6 and 7 show the diurnal variation of the incoming and outgoing longwave fluxes as observed and modeled with MYSTIC. The agreement of the observed and modeled incoming longwave fluxes is very good: the mean difference in the diurnal variation between 15 MST and 09 MST does not exceed 10 W m^{-2} at any of the 6 sites. The differences are mainly due to offsets, as indicated by standard deviations of the differences of less than 3.5 W m^{-2}.

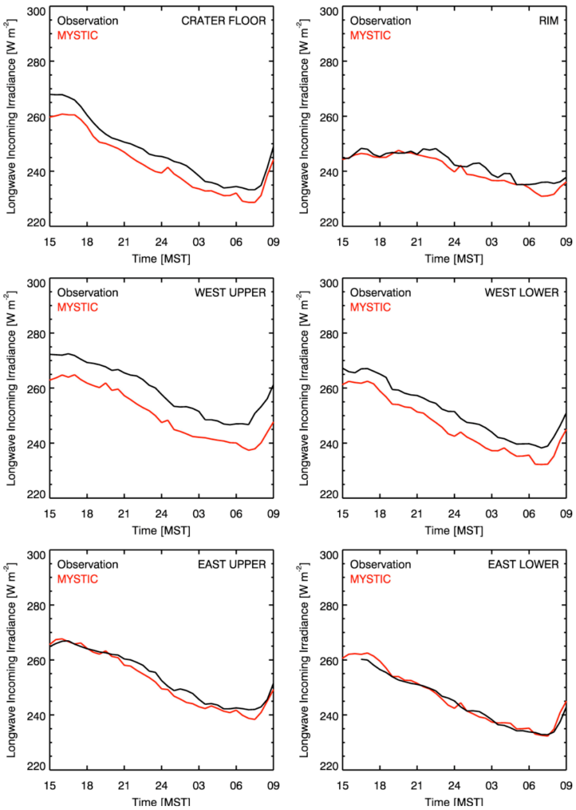

Fig. 6: Comparison of observed (black) and modeled (red) longwave incoming radiation at the six crater sites for the night of 22 - 23 October 2006.

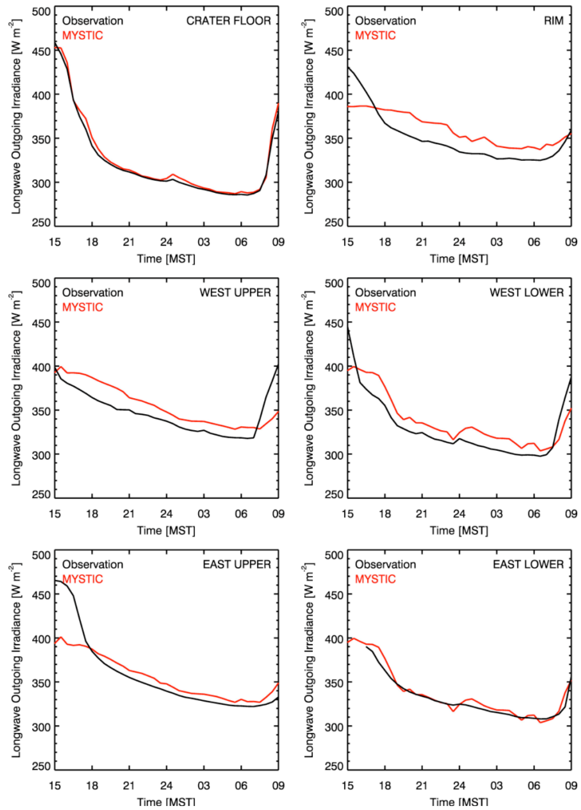

Fig. 7: Comparison of observed (black) and modeled (red) slope-parallel longwave outgoing radiation at the six crater sites for the night of 22 - 23 October 2006.

Differences between the modeled and observed outgoing fluxes are more apparent, but they are site specific. At Floor, the overall agreement is very good – which is to be expected as the temperature input to the model is compiled from data taken not far away from the observation. At all other sites the model tends to overestimate the outgoing radiation during the night. This is attributed to the before-mentioned near surface inversions over the slopes of the crater topography that are not resolved with the 1D temperature profile observed over the crater center. Accordingly, shallow superadiabatic layers that exist over the sunlit slopes in the afternoon and during post-sunrise periods are not resolved by the model. An underestimation of the outgoing longwave flux is seen at these times, for example at West Upper and West Lower between 07 and 09 MST and between 15 and 17 MST at East Upper (no observation data at East Lower at this time).

5. TOPOGRAPHIC EFFECTS ON THE RADIATION BALANCE

Because MYSTIC performed well in simulating radiation observations in the basin, a second step was taken – to make parametric simulations with MYSTIC focused on gaining improved understanding of the influences of atmospheric stability and air-ground temperature differences on the radiation field within the crater. For this purpose, the 18 MST sounding was modified so that an isothermal and constant mixing ratio atmosphere extended down into the crater from an elevation 500 m above the crater floor. The temperature of the lowest 500 m layer was 10°C and the mixing ratio was 2.1 g/kg. Parametric simulations were then performed in which temperature differences of 0°C, +20°C and -20°C were imposed at the surface between the air and ground temperatures. In a second set of simulations, the atmospheric stability of the lowest 500 m layer was changed from isothermal to +5 K/100m. The results are shown in terms of transects across the crater from south to north along the line shown in Figure 1. The calculations were made for all grid elements along this transect.

Figure 8 shows results for the isothermal atmosphere with the three air-ground temperature discontinuities on a south-north transect across the crater. An enhanced (reduced) topographic effect on the downward longwave radiation is seen when the surface temperature is increased (decreased) relative to the temperature of the air. The topographic effect varies with slope angle. The double "spike" in the transect across the north rim indicates this relationship. The spikes appear where the terrain exhibits steep sections and the terrain surface area in the field of view of the instruments increases. The upward longwave flux shows no widespread topographic effect. Only the increase (de-

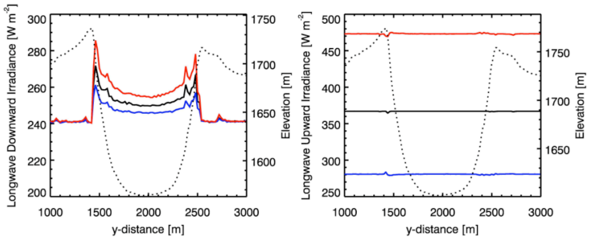

Fig. 8: Modeled longwave downward (left) and upward (right) fluxes at 2 m above the topography under isothermal atmospheric stratification. Black: Surface temperature same as air temperature. Blue: Surface temperature 20 K colder than air temperature. Red: Surface temperature 20 K warmer than air temperature. Fluxes are represented by the scales on the left. Elevation cross sections are shown as thin dotted lines with the scale given on the right.

crease) with higher (lower) surface temperature according to the Stefan-Boltzmann Law is seen.

Figure 9 illustrates the effects of differing atmospheric stability on the longwave flux transects. The mean longwave downward flux decreases under stable stratification. Also, the variation along the flux transect is reduced under stable conditions. When moving along the transect toward the crater floor a compensating effect comes into play - the increase in flux caused by the larger contribution from terrain-emitted radiation is reduced when this contribution originates from terrain with colder surface temperatures. Colder surface temperatures are found at the lower elevations in a stable atmosphere. Thus, the incoming flux at the bottom of the crater can be lower than the incoming flux on the plain. The outgoing flux is determined by the temperature distribution following the Stefan-Boltzmann Law. With an assumption of a linear distribution of temperature with terrain, the flux transect mirrors the crater topography.

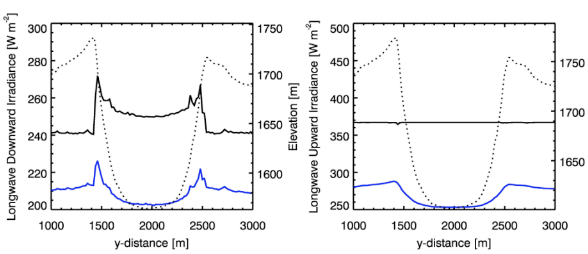

Fig. 9: Modeled longwave downward (left) and upward (right) fluxes 2 m above the topography under different atmospheric stratifications, isothermal (0 K/100 m, black) and stable (5 K/100 m, blue). The surface temperature was set to the temperature of the adjacent air. Flux values are shown on the left scale, while elevation values for the terrain cross section (thin dotted line) are shown on the right.

6. CONCLUSION

Observations during METCRAX were used to validate the MYSTIC 3D radiative transfer model. MYSTIC provides accurate simulations of the topographic effects of terrain shading, terrain exposure and terrain reflection on the shortwave fluxes. Model calculations under different atmospheric stratifications and surface temperature boundary conditions allow the quantification of the influence of topography on the longwave energy balance.

Future research with MYSTIC will include the calculation of radiative heating rates within the crater basin under varying atmospheric conditions. Parametric studies will address the influences of basin size and shape.

Acknowledgements: SWH was supported by an Individual Support Fellowship from the Swiss National Science Foundation and ARO Grant 52734-EV. CDW was supported by National Science Foundation grant ATM-0444205. We thank the Barringer Crater Company (D. Barringer, Pres.) and Meteor Crater Enterprises, Inc. (B. Andes, Pres.) for crater access. We appreciate the field assistance of M. Hahnenberger, S. Zhong, and others. We especially would like to thank the NCAR field personnel who assisted with the radiation data, including S. Oncley, T. W. Horst, W. O. J. Brown, G. Maclean, C. Martin, J. Militzer, and S. Semmer.

REFERENCES

Hoch, S. W., and C. D. Whiteman, 2007: The surface radiation balance in and around Arizona's Meteor Crater. 29th Intl Conf. Alpine Meteor., 4-8 June 2007, Chambéry, France.

Matzinger, N., M. Andretta, E. Van Gorsel, R. Vogt, A. Ohmura, and M. W. Rotach, 2003: Surface radiation budget in an Alpine Valley. *Quart. J. Roy. Meteor. Soc.*, **129**, 877-895.

Mayer, B., 1999: I3RC phase 1 results from the MYSTIC Monte Carlo model. Extended abstract for the I3RC (Intercomparison of 3D radiation codes) workshop, Tucson, Arizona, November 17-19, 1999.

Mayer, B. and A. Kylling, 2000a: Three-dimensional radiative transfer calculations with the MYSTIC model. Poster presentation at IRS 2000, St. Petersburg, Russia, 24 - 29 July 2000.

Mayer, B. and A. Kylling, 2000b: Three-dimensional radiative transfer calculations with the MYSTIC model. Presentation at EGS 2000, Nice, France, 25 - 29 April 2000.

Mayer, B., and A. Kylling: 2005: Technical note: The libRadtran software package for radiative transfer calculations – Description and examples of use. *Atmos. Chem. Phys.*, **5**, 1855-1877

Whiteman, C. D., K. J. Allwine, L. J. Fritschen, M. M. Orgill, and J. R. Simpson, 1989: Deep valley radiation and surface energy budget microclimates. Part I: Radiation. *J. Appl. Meteor.*, **28**, 414-426.

Whiteman, C. D., A. Muschinski, S. Zhong, D. Fritts, S. W. Hoch, M. Hahnenberger, W. Yao, V. Hohreiter, M. Behn, and Y. Cheon, C. B. Clements, T. W. Horst, W. O. J. Brown, and S. P. Oncley, 2008: METCRAX 2006 – Meteorological experiments in Arizona's Meteor Crater. *Bull. Amer. Meteor. Soc.* In press